Absolute differential and integral cross sections for charge transfer of keV O^+ with N_2

B. G. Lindsay, R. L. Merrill, H. C. Straub, K. A. Smith, and R. F. Stebbings
Department of Space Physics and Astronomy, Department of Physics, and Rice Quantum Institute, Rice University, 6100 Main Street, Houston, Texas 77005-1892
(Received 29 August 1997)

We report measurements of the absolute differential cross sections for charge transfer scattering of 0.5-, 0.85-, 1.5-, 2.8-, and 5-keV O^+ by N_2 at scattering angles between 0.04° and 3.1° in the laboratory frame. Cross sections for both $O^+(^4S)$ ground-state and $O^+(^2D,^2P)$ metastable projectiles are presented. The ground-state cross section is much smaller than that for the metastable state and the influence of the electronic state of the projectile on the angular distribution of the scattered neutrals is also very significant. The estimated total cross sections are compared with previous measurements. [S1050-2947(98)08401-7]

PACS number(s): 34.70.+e, 34.50.Lf

INTRODUCTION

Charge transfer of O^+ with N_2 has been of interest from a fundamental atomic physics point of view for a number of years. This is because the cross section is known to depend markedly on the initial electronic state of the oxygen ion [1–5]. The explanation normally given for this is that the $O^+(^2D)$ metastable excited state is essentially in energy resonance with the $N_2^+(A\ ^2\Pi_u)$ state and the cross section is therefore large but there is approximately 2 eV between the $O^+(^4S)$ ground-state energy and that of the nearest N_2^+ state ($X\ ^2\Sigma_g^+$) and that cross section is therefore much smaller. The $O^+(^2P)$ metastable excited state is also near resonant with N_2^+ [6].

Charge transfer of oxygen ions with N_2 is likewise important in the field of aeronomy [7,8]. O^+ is the dominant ion in the *F* region of the atmosphere and both metastable species have been detected there. Satellite measurements have also observed keV O^+ ions precipitating into the earth's atmosphere during periods of geomagnetic activity [9]. The energy carried by these ions can be quite large and can significantly influence the behavior of the upper atmosphere. The detailed behavior of the precipitating O^+ flux depends critically on the magnitude of the various charge changing cross sections. Efforts to model the effect of this precipitation on the atmosphere have been hampered by a lack of accurate experimental data, causing modelers to rely on theoretical predictions [10–15]. The angular distribution of the scattered neutral charge transfer products, which influences how far the precipitating fluxes may penetrate into the atmosphere [7] and is required to understand this process quantitatively, has so far not even been addressed theoretically.

Despite the study which charge exchange of O^+ with N_2 has received there is still doubt as to the magnitude of the cross sections. The uncertainties quoted by several of the early investigators were significant and the various measurements are not always in adequate agreement. There has also been no previous work on the relationship of the differential cross section (DCS) for this reaction to the electronic state of the projectile. From theoretical considerations the DCS ought to have a strong dependence on the projectiles' degree of excitation. This paper reports measurements of the differential and integral cross sections for both ground-state and metastable O^+ and, where possible, the total charge exchange cross sections have also been determined. These total cross sections are compared to those available in the literature.

There are two low-lying metastable excited states of O^+, ^2D and ^2P, with lifetimes of approximately 3.6 h and 5 s, respectively [16]. In early studies it has often been stated that the observed metastable ions are $O^+(^2D)$ [2,3,17]. However, recently it has been shown [18] that not only are both metastable ions readily produced by electron impact ionization of O_2 (as used in this work) but that the charge exchange cross sections for these species with N_2 are similar at projectile energies of 15 eV or so [6] and presumably are even closer at the energies employed here. While all the observations made during this investigation are consistent with only one metastable component, which would presumably be $O^+(^2D)$, given the recent findings of Lavollée and Henri [6], it is likely that the techniques used in this study would not be sufficiently sensitive to differentiate between the two metastable species. Therefore, without further evidence, the metastable ions used for this study are identified as some unknown mix of $O^+(^2D)$ and $O^+(^2P)$.

APPARATUS AND EXPERIMENTAL METHOD

A schematic of the scattering apparatus is shown in Fig. 1. Positive ions emerging from a low-pressure plasma-type ion source containing oxygen are accelerated to the desired energy and focused by an electrostatic lens. The ions are then

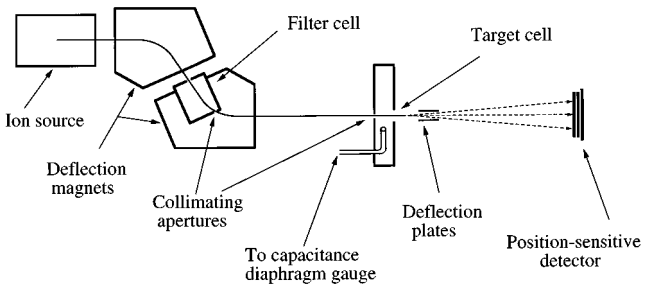

FIG. 1. Schematic of the apparatus.

mass selected by a pair of 60° sector magnets and the O^+ beam passes through a ''filter cell,'' containing N_2, and a collimating aperture before traversing the target cell. This collimating aperture together with the entrance aperture of the target cell defines the angular divergence of the ion beam. The filter cell is configured in such a manner that the fast neutral O atoms which are generated by charge exchange with the filter cell gas cannot enter the target cell. Both the filter cell pressure and the target cell pressure are monitored using capacitance diaphragm gauges. A position-sensitive detector (PSD) on the beam axis 26 cm beyond the target cell is used to monitor both the primary ion beam and the fast neutral collision products. When making cross-section measurements the pressure in the target cell is chosen to ensure single collision conditions and the differential cross section for charge exchange is then given by

$$\frac{d\sigma(\theta)}{d\Omega}=\frac{\Delta S(\theta)}{Snl\Delta\Omega}, \tag{1}$$

where S is the primary ion beam flux, $\Delta S(\theta)$ is the neutral flux scattered at angle θ into a solid angle $\Delta\Omega$, n is the target number density, and l is the target cell length. $\Delta S(\theta)$ is determined by applying a transverse electric field to deflect the O^+ beam after it passes through the target cell thereby allowing only the neutral collision products to impact the PSD. To measure the ion beam flux (typically a few thousand particles per second) this field is momentarily removed. The resulting flux of ions and neutrals is equal to S, the flux of ions entering the target cell. As the PSD has only a limited acceptance angle, the few neutrals which are scattered by large angles do not impact it, however, as only a small fraction of the incident ion beam undergoes charge exchange and only a small fraction of the resulting neutrals are scattered at large angles their effect is generally negligible. The PSD output is therefore a measure of S because, as discussed below, the ions and neutrals are detected with the same efficiency. During this measurement, the ion beam is rastered over a 0.5×0.5 cm square on the detector to ensure that the detection efficiency is not impaired by saturation effects that occur when only a few microchannels are impacted by an intense highly collimated ion beam [19]. As indicated in Eq. (1), cross-section determination involves measurement of the ratio of the fluxes of the primary ions and neutral products. Previous studies in this laboratory [20,21] have shown that the ion and neutral detection efficiencies are identical within the experimental uncertainties at 5 keV while at 1.5 and 0.5 keV they are the same to within 5% and 10%, respectively. In this work, therefore, we take $\Delta S/S$ as equal to the ratio of the neutral signal to ion signal recorded by the PSD.

Since the target species are not oriented in any way, the product scattering pattern is symmetric about the beam axis. The origin of the coordinate system for analysis of the scattering is identified with the ''center of mass'' of the distribution and the detector area is partitioned into a set of rings concentric with this origin. The angular displacement of each ring and the solid angle it subtends at the target cell are established by the geometry of the apparatus. Effects due to scattering by residual gas and apertures are removed by an appropriate background subtraction. A more detailed description of the apparatus and the analysis method has been given in a previous publication [22].

CROSS-SECTION DETERMINATION

A number of studies have been completed in this laboratory involving various target gases and cross sections obtained by use of Eq. (1) have been reported. In the present investigation this approach has been modified in order that the individual cross sections for the ground-state and metastable ions may be obtained. The determination of state selected cross sections is generally quite difficult and the techniques employed range from the conceptually straightforward beam attenuation method developed by Stebbings, Turner, and Rutherford [1] and Turner, Rutherford, and Compton [17] to more elaborate contemporary methods such as the triple-quadrupole double-octopole technique of Li *et al.* [23]. The technique employed here has evolved from that originally developed by Stebbings, Turner, and Rutherford [1], which has been described in detail by Turner, Rutherford, and Compton [17]. The basis of this technique is as follows. A beam of identical particles is attenuated in passing through a gas according to the simple attenuation law

$$I=I_0e^{-nl\sigma}, \tag{2}$$

where I is the beam intensity, I_0 is the initial intensity of the beam, σ is the cross sections for removal of a particle from the beam, l is the length through which the beam passes, and n is the number density of the gas. A beam containing two different components will likewise be attenuated according to

$$I=I_1e^{-nl\sigma_1}+I_2e^{-nl\sigma_2}, \tag{3}$$

where I_1 and I_2 are the initial intensities of components (1) and (2) and σ_1 and σ_2 are their cross sections for removal from the beam. In circumstances where σ_1 and σ_2 are sufficiently different it is possible, by determining the attenuation of the beam as a function of n, to obtain the fraction of ions initially in each state and the separate cross sections. Furthermore, it is also possible to preferentially remove those particles having the larger cross section from the beam.

It was observed by Stebbings, Turner, and Rutherford [1] that the attenuation of a beam of O^+ ions in passing through a target of O_2 or N_2 could indeed be expressed as the sum of two exponentials as in Eq. (3) thereby giving clear evidence of the presence of two different components in the ion beam. They concluded that the O^+ beam was comprised of both ground-state and long lived metastable ions. Although there was some attenuation of the beam as a consequence of elastic collisions, charge exchange was the predominant mechanism by which ions were removed from the beam. Analysis of the attenuation curve permitted evaluation of the fraction of ions initially in each state and the separate cross sections. The observations of Stebbings, Turner, and Rutherford [1] suggested that the metastable component comprised ^2D ions alone and subsequent researchers have often agreed with this interpretation. However, as has been noted in the introductory section of this paper, if $O^+(^2D)$ and $O^+(^2P)$ ions

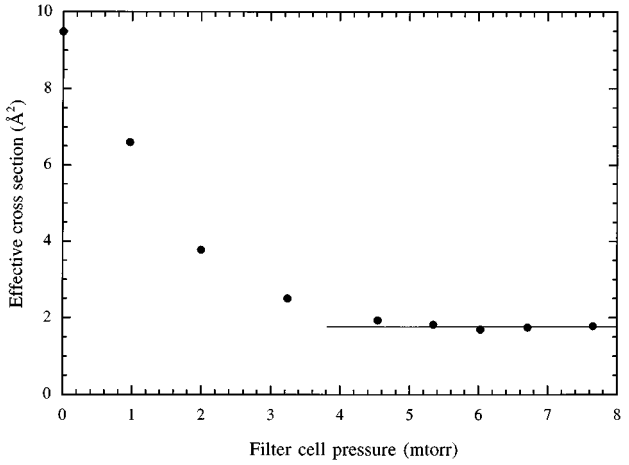

FIG. 2. Effective integral O^+-N_2 charge transfer cross section as a function of filter cell pressure. The data shown are for 1.5-keV O^+ projectiles and the filter gas used was N_2.

should have similar charge exchange cross sections then they would be essentially indistinguishable.

In the present work the $O^+(^4S)$ cross section was obtained by increasing the N_2 pressure in the filter cell until almost all of the $O^+(^2D,^2P)$ ions had been converted to neutrals by charge exchange and the emerging O^+ beam therefore consisted essentially of ground-state ions. N_2 was then admitted to the target cell and the cross section for this beam was measured using the techniques outlined earlier. The operating conditions necessary to obtain a ground-state ion beam were determined by plotting the effective cross section [i.e., the charge transfer cross section for the ion beam containing some admixture of $O^+(^4S)$ and $O^+(^2D,^2P)$ with an N_2 target] as a function of the filter cell pressure as shown in Fig. 2. With no gas in the filter cell the measured effective cross section is approximately 10 $Å^2$; as the N_2 pressure in the filter cell is increased, it falls rapidly and finally converges to the ground-state cross section. It is estimated that for the data shown in the figure, at pressures greater than 6 mtorr, more than 99% of the O^+ ions emerging from the filter cell were in the ground state.

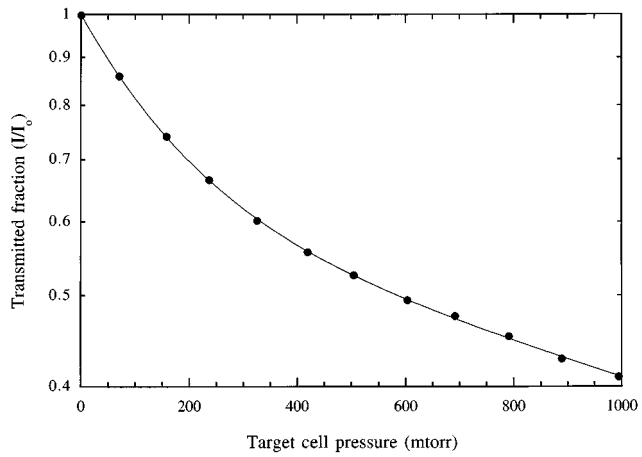

FIG. 3. A typical attenuation curve for 1.5-keV O^+ projectiles incident on N_2. The solid line is a two-component exponential fit to the data. Note that the y axis is logarithmic.

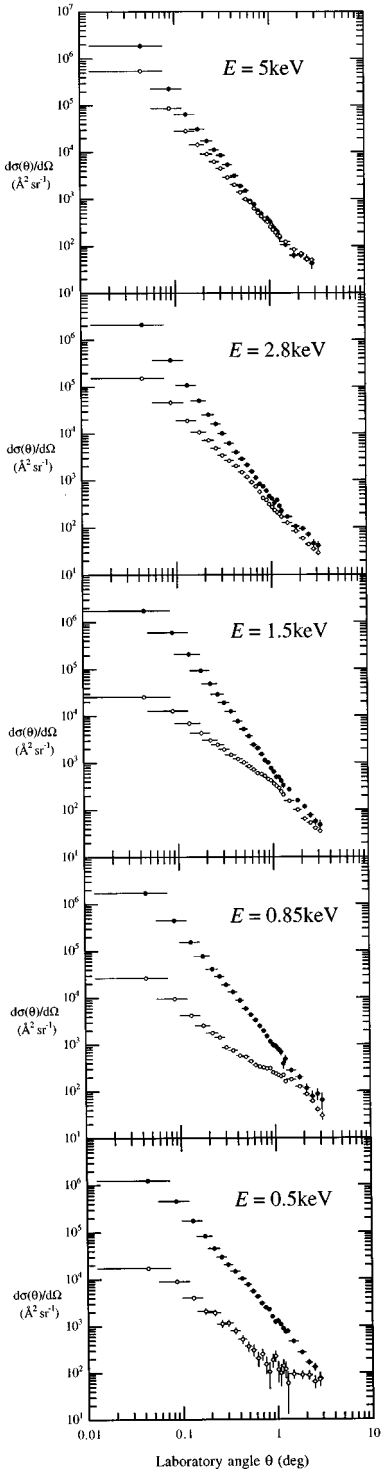

FIG. 4. Absolute differential cross sections for charge transfer scattering of $O^+(^4S)$ by N_2 (hollow circles) and $O^+(^2D,^2P)$ by N_2 (filled circles) at the projectile energies indicated.

The $O^+(^2D,^2P)$ cross section was determined by evacuating the filter cell, then measuring the effective cross section for the mixed composition beam, determining the fraction of ions in the ground state, and subtracting the contribution these ground-state ions would have made to the total scattering signal. Normally the effective cross-section measurement and two fraction measurements were made within less than

TABLE I. Laboratory frame differential charge transfer cross sections for $O^+(^4S)$-N_2 collisions, where E is the projectile energy and the numbers in square brackets represent powers of 10.

Laboratory angle θ	$d\sigma(\theta)/d\Omega$ (Å^2 sr^{-1})				
(deg)	$E=0.5$ keV	$E=0.85$ keV	$E=1.5$ keV	$E=2.8$ keV	$E=5$ keV
0.044	1.72[4]	2.63[4]	2.57[4]	1.55[5]	5.50[5]
0.087	8.99[3]	9.57[3]	1.28[4]	4.61[4]	8.72[4]
0.131	4.00[3]	4.24[3]	7.01[3]	1.90[4]	2.82[4]
0.175	2.08[3]	2.55[3]	4.37[3]	1.08[4]	1.45[4]
0.218	1.93[3]	1.77[3]	3.08[3]	7.23[3]	9.18[3]
0.262	1.12[3]	1.43[3]	2.48[3]	4.92[3]	6.28[3]
0.306	1.16[3]	8.71[2]	1.96[3]	3.46[3]	4.53[3]
0.360	7.89[2]	7.53[2]	1.50[3]	2.66[3]	2.91[3]
0.426	5.22[2]	5.76[2]	1.22[3]	2.03[3]	2.04[3]
0.491	3.71[2]	5.48[2]	1.04[3]	1.50[3]	1.41[3]
0.557	3.09[2]	4.37[2]	8.57[2]	1.18[3]	1.01[3]
0.622	2.07[2]	3.66[2]	7.30[2]	9.23[2]	8.71[2]
0.688	2.52[2]	3.34[2]	6.05[2]	7.40[2]	6.41[2]
0.753	1.54[2]	3.20[2]	5.76[2]	5.70[2]	5.10[2]
0.819	1.04[2]	3.04[2]	5.29[2]	4.24[2]	4.35[2]
0.884	1.88[2]	3.08[2]	4.59[2]	3.82[2]	3.88[2]
0.950	2.30[2]	2.54[2]	4.22[2]	3.11[2]	3.28[2]
1.02	1.16[2]	2.38[2]	3.65[2]	2.74[2]	2.58[2]
1.08	9.85[1]	2.20[2]	3.26[2]	2.36[2]	2.24[2]
1.15	1.42[2]	2.07[2]	2.96[2]	2.10[2]	1.98[2]
1.21	1.21[2]	2.20[2]	2.48[2]	1.95[2]	1.69[2]
1.28	5.94[1]	1.60[2]	2.11[2]	1.68[2]	1.64[2]
1.47	9.34[1]	1.77[2]	1.55[2]	1.28[2]	1.24[2]
1.80	9.06[1]	1.25[2]	1.00[2]	8.50[1]	8.46[1]
2.13	8.96[1]	8.57[1]	6.49[1]	5.94[1]	6.96[1]
2.46	6.45[1]	6.15[1]	5.35[1]	4.40[1]	5.17[1]
2.78	7.20[1]	4.06[1]	4.08[1]	3.53[1]	3.63[1]
3.11		3.00[1]	3.55[1]	2.92[1]	

an hour. The fraction of ions in the ground state was initially measured using the attenuation technique of Stebbings, Turner, and Rutherford [1], however, because of ion beam instability, this proved both time consuming and difficult. Therefore a modified version of this technique was developed which is much less sensitive to beam instability and which inherently yields more precise data than the original. This approach again entails an attenuation curve measurement, however, the ion beam flux entering the target cell is now monitored as the attenuation curve data are being acquired. The attenuation curve is obtained by varying the N_2 pressure in the target cell rather than that in the filter cell, which remained evacuated during the measurement. This permits ions and neutrals which pass through the target cell to be detected on the PSD. The attenuation of the ion beam, by charge exchange, as it passed through the target cell is determined by observing the sum of the ion and neutral signals, which is a measure of the incident ion flux, then deflecting the ions and observing the neutral signal alone. The flux of transmitted ions is then the difference of these two values. During attenuation measurements the ''ion plus neutral'' signal and the neutral signal are both sampled every two seconds. A typical attenuation curve is shown in Fig. 3. The fitting equation assumes that the beam consists of only ions in the ground state and one metastable state. The excellent fits obtained tend to confirm this two-component analysis. If, however, both metastable ions have similar cross sections as has been postulated earlier then equally good fits would be found. In contrast to the O^+-N_2 case it was found that the attenuation of a ground-state He^+ beam by He gave an excellent single exponential fit.

Extensive testing was performed to establish the accuracy of the modified attenuation technique and the cross sections derived by employing it. The new technique gave ground-state fractions that were in agreement with the traditional attenuation method to within $\pm 3\%$ at 5 keV, $\pm 8\%$ at 1.5 keV, and $\pm 9\%$ at 0.5 keV. Furthermore, the measured integral metastable-state charge exchange cross section, which is almost directly dependent on the measured metastable fraction, was found to be the same to within 5% when the metastable fraction in the primary beam was varied from 20% to 40% by deliberately changing the source conditions. Integral cross-section measurements made at different times were also found to be at least as consistent.

RESULTS AND DISCUSSION

The DCS's for charge transfer of $O^+(^4S)$ and $O^+(^2D,^2P)$ with N_2 at 0.5, 0.85, 1.5, 2.8, and 5 keV are shown in Fig. 4

TABLE II. Laboratory frame differential charge transfer cross sections for $O^+(^2D,^2P)$-N_2 collisions, where E is the projectile energy and the numbers in square brackets represent powers of ten.

Laboratory angle θ	$d\sigma(\theta)/d\Omega$ (Å^2 sr^{-1})				
(deg)	$E=0.5$ keV	$E=0.85$ keV	$E=1.5$ keV	$E=2.8$ keV	$E=5$ keV
0.044	1.24[6]	1.73[6]	1.74[6]	2.14[6]	1.89[6]
0.087	4.57[5]	4.48[5]	5.97[5]	3.72[5]	2.30[5]
0.131	1.75[5]	1.55[5]	2.09[5]	1.09[5]	6.50[4]
0.175	8.30[4]	7.76[4]	9.36[4]	5.05[4]	3.15[4]
0.218	4.54[4]	4.11[4]	4.92[4]	2.54[4]	1.77[4]
0.262	2.96[4]	2.88[4]	2.93[4]	1.61[4]	1.13[4]
0.306	2.03[4]	1.91[4]	1.91[4]	1.01[4]	8.64[3]
0.360	1.46[4]	1.34[4]	1.25[4]	6.24[3]	5.43[3]
0.426	1.03[4]	8.82[3]	7.74[3]	4.00[3]	3.15[3]
0.491	7.68[3]	5.90[3]	5.27[3]	2.88[3]	1.91[3]
0.557	5.55[3]	4.37[3]	3.74[3]	2.13[3]	1.53[3]
0.622	4.28[3]	3.37[3]	2.44[3]	1.53[3]	9.11[2]
0.688	3.08[3]	2.51[3]	2.09[3]	1.14[3]	7.72[2]
0.753	2.48[3]	1.98[3]	1.55[3]	8.40[2]	5.62[2]
0.819	2.27[3]	1.52[3]	1.13[3]	7.48[2]	4.87[2]
0.884	1.60[3]	1.17[3]	1.01[3]	5.97[2]	3.72[2]
0.950	1.23[3]	9.92[2]	7.72[2]	4.62[2]	3.87[2]
1.02	1.30[3]	9.20[2]	6.48[2]	4.12[2]	3.29[2]
1.08	1.10[3]	8.08[2]	5.05[2]	3.33[2]	2.60[2]
1.15	8.90[2]	6.99[2]	4.97[2]	3.84[2]	2.24[2]
1.21	7.62[2]	3.92[2]	4.16[2]	2.86[2]	1.96[2]
1.28	7.80[2]	4.94[2]	3.31[2]	2.25[2]	1.53[2]
1.47	4.73[2]	2.80[2]	2.73[2]	1.69[2]	1.07[2]
1.80	2.75[2]	2.00[2]	1.58[2]	1.07[2]	6.39[1]
2.13	1.68[2]	1.16[2]	1.17[2]	9.53[1]	6.42[1]
2.46	1.32[2]	7.75[1]	7.75[1]	7.16[1]	5.56[1]
2.78	7.61[1]	8.74[1]	5.67[1]	4.64[1]	4.27[1]
3.11		6.45[1]	4.84[1]	4.16[1]	

and tabulated in Tables I and II. The vertical error bars in the figure represent the statistical error only. The horizontal error bars arise from the finite primary beam size and the ''ring'' width used for analysis and are thus primarily an indication of the angular resolution of the measurement. The DCS's for 0.5- and 5-keV projectiles at the most extreme scattering angle are absent due to count rate and background problems at the limits of the working range of the apparatus. All of the metastable cross sections are very forward peaked, as would be expected for a near resonant process; the ground-state cross sections, however, are not only much smaller in magnitude but also show a very different angular dependence. This is most obvious at small angles. The ground- and metastable-state small angle differential cross sections at 0.5-keV impact energy differ by almost two orders of magnitude. As the impact energy is increased, the ground-state cross section becomes much closer to the metastable cross section, both in form and magnitude. This is due to the fact that charge exchange with the ground state is relatively unlikely at low impact energy, because the approximately 2 eV that is required for the ground-state reaction to proceed must come from the kinetic energy of the incident ion, but as the kinetic energy is increased, this 2 eV becomes a smaller fraction of the impacting ions' kinetic energy and is thus more easily accessible. Another way of understanding the behavior of these differential cross sections is to consider that in order to transfer sufficient kinetic energy to internal energy (to facilitate the charge exchange reaction) impacting ground-state ions must make relatively hard collisions and they will thus scatter at relatively large angles. The DCS for ground-state O^+ will therefore tend to be spread over a larger angular range than that for the metastables. This behavior is clearly evident from the figure. It must be noted that because of the huge disparity in magnitude between the small angle DCS's for the $O^+(^4S)$ and $O^+(^2D,^2P)$ ions and because it was not possible to obtain a 100% pure ground-state beam the value of the ground-state differential cross section below approximately 0.1° at the three lowest projectile energies should only be considered an upper limit. No other experimental or theoretical data exist with which to compare these differential cross sections.

A comparison with earlier measurements of the total cross sections is made in Fig. 5, perhaps the most striking feature of which is the large difference in magnitude of the ground-state and metastable cross sections. In the present experiment it was only possible to measure the integral cross sections, which are given in Table III, and it was therefore necessary to perform a simple power-law extrapolation in order to obtain an estimate of the total cross sections. As the metastable cross sections are so forward peaked the integral cross-

TABLE III. Absolute O^+-N_2 charge transfer cross sections. The angular range for the integral cross sections is 0°–3.3°.

	Absolute integral cross section (Å^2)		Absolute total cross section (Å^2)	
Projectile energy (keV)	$O^+(^4S)$	$O^+(^2D,^2P)$	$O^+(^4S)$	$O^+(^2D,^2P)$
0.50	1.2±0.2	19.7±3.6		21.9±4.0
0.85	1.5±0.3	20.1±3.6	2.3+2.0,−0.8	21.1±3.8
1.5	1.8±0.2	21.2±3.4	3.0±1.1	21.9±3.5
2.8	3.1±0.3	18.5±1.8	5.0±1.9	21.3±3.4
5.0	5.7±0.9	15.9±2.5	8.6±2.9	16.2±2.6

section values presented here are very close to the total cross sections, the maximum difference being only about 15%. This is, however, not the case for the integral ground-state data where a significant fraction of the neutral products do not impact the PSD. It is difficult to quantify the overall accuracy of the ground-state extrapolation and therefore the uncertainties shown in the figure are somewhat conservative. It was not possible to obtain any meaningful estimate of the total ground-state cross section at 0.5 keV using this extrapolation technique.

The data presented in Fig. 5 were obtained by a variety of experimental methods. The experiments fall into two broad classes; those in which the cross section is determined from measurements of the slow product ions and those in which the fast neutral products are detected. In principle these two approaches lead to the same result. Stebbings, Turner, and Rutherford [1], Rutherford and Vroom [2], Flesch and Ng [24] and Li *et al.* [23] all observed the slow product ions. The fast neutral products were detected by Moran and Wilcox [3], Hoffman, Miller, and Lockwood [5], and the present study. Flesch and Ng [24] and Li *et al.* [23] were able to determine the cross section for production of N_2^+ and that for N^+, i.e., the cross section for dissociative charge exchange, and their data have therefore been presented as the sum of these two cross sections.

The various studies can also be distinguished by the particular technique used to obtain the state specific cross section. For the case of ground-state O^+ ions four separate methods have been employed. Moran and Wilcox [3] and Hoffman, Miller, and Lockwood [5] utilized a controlled electron impact ion source to produce a pure $O^+(^4S)$ ground-state beam, Flesch and Ng [24] produced their ground-state ions by dissociative photoionization of O_2, Li *et al.* [23] used a combination of dissociative charge transfer and rf octopole ion trap, and in this study the ground-state ion beam was obtained by filtering out the metastable component from a mixed-state beam. The metastable-state work has relied on one of three general methods, Stebbings, Turner, and Rutherford [1], Moran and Wilcox [3], and the present study measured the cross section for a mixed-state ion beam and then used the fractional abundance of ground-state and metastable ions in that beam to determine the cross section for the metastable component. Rutherford and Vroom [2] prepared their O^+ ions by dissociative charge exchange and determined the abundance of $O^+(^2D)$ ions based on the observation that $O^+(^2D)$ has a small cross section for formation of NO^+. The most recent metastable measurement, that of Li *et al.* [23], also used dissociative charge exchange but in combination with a technique based on the rf octopole ion trap.

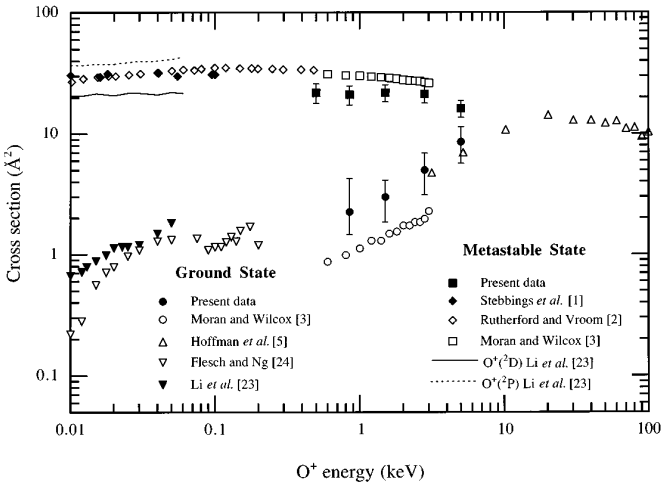

FIG. 5. Absolute O^+-N_2 total charge transfer cross sections.

The present ground-state total cross sections are in excellent agreement with those of Hoffman, Miller, and Lockwood [5] whose stated uncertainty is ±10%, and also with a simple extrapolation of the measurements of Flesch and Ng [24] and Li *et al.* [23] whose absolute uncertainties are ⩽20% and ⩽25%, respectively. The ground-state data of Moran and Wilcox [3], which has an uncertainty similar to that of Hoffman, Miller, and Lockwood [5], lie significantly lower than the present total cross sections. It is noteworthy that recent measurements of the charge transfer cross section for $O^+(^4S)$ with H_2 by other investigators also lie higher than the relevant Moran and Wilcox [3] data [25,26].

The present $O^+(^2D,^2P)$ total cross section is somewhat lower than that of the other investigators. It is, however, rather difficult to compare the various data sets as it is unclear exactly what the uncertainties are in much of the earlier data. Stebbings, Turner, and Rutherford [1] state that their data are good to better than a factor of 2; Rutherford and Vroom [2] do not state explicitly how accurate they believe their data to be, however, as their apparatus was substantially the same as that used by Stebbings, Turner, and Rutherford [1] it seems reasonable to assume an uncertainty of similar magnitude. Moran and Wilcox [3] state that the absolute error associated with their cross sections is approximately ±7% due to uncertainties in the absolute determination of the target gas concentration and the assessment of their neutral beam flux. They do not, however, state the accuracy of

the ground- and metastable-state fractions used in their work which are crucial to the determination of the metastable cross section. However, as Turner, Rutherford, and Compton [17], from whom Moran and Wilcox [3] derived their ground-and metastable-state fractions, clearly state that the fractions which they quote in their publication strictly apply only to the experimental configuration used in that work, it seems clear that there must be a considerable degree of uncertainty associated with the procedure used by Moran and Wilcox [3]. In support of this argument, we found during this experiment that the measured metastable fraction depended markedly on the conditions under which the ion source was operated.

The recent low-energy $O^+(^2D)$ data of Li *et al.* [23] have a smaller absolute uncertainty than the older measurements, $\leqslant 25\%$. The data which are shown in the figure supersede a previous measurement by Flesch and Ng [27]. These data are in agreement with the work of Stebbings, Turner, and Rutherford [1] and Rutherford and Vroom [2] to within their uncertainties. The data of Li *et al.* [23] can also be directly compared to that of Lavollée and Henri [6] (not shown), who used an approach derived from the threshold photoelectron-photoion coincidence technique. The work of Lavollée and Henri [6] is in agreement with the Li *et al.* [23] study as to the absolute $O^+(^2D)$ cross section, which Lavollée and Henri estimate to be approximately 25 $Å^2$ at these energies. However, Lavollée and Henri [6] found the ratio of the $O^+(^2P)$ cross section to that for $O^+(^2D)$ to be 0.6 at energies between 8 and 20 eV whereas Li *et al.* [23] found that the $O^+(^2P)$ cross section was larger than that for $O^+(^2D)$ (Fig. 5). Consequently, it is probably premature to assume that the low-energy metastable cross sections are known to much better than the factor of 2 of the older measurements.

In summary, the present data for both $O^+(^4S)$ and $O^+(^2D,^2P)$ agree with the older measurements to within the uncertainties of those data [except for the $O^+(^4S)$ data of Moran and Wilcox [3]] and are not inconsistent with the more recent low-energy studies. Given the uncertainty that is still associated with the values of these cross sections there is evidently further work to be done on this problem.

CONCLUSION

The absolute differential cross sections for charge transfer scattering of 0.5-, 0.85-, 1.5-, 2.8-, and 5-keV $O^+(^4S)$ and $O^+(^2D,^2P)$ by N_2 at scattering angles between 0.04° and 3.1° in the laboratory frame have been determined. The ground-state cross section is very much smaller than that for the metastable state and the effect of different electronic states of the projectile on the angular distribution of the scattered neutrals is very significant. These results are both of fundamental interest and have potential application in the field of aeronomy. The most reliable previous total cross-section measurements are in good agreement with those reported here. Future work will involve making similar measurements for O_2 and H_2 targets.

ACKNOWLEDGMENTS

We gratefully acknowledge support by the Atmospheric Sciences Section of the National Science Foundation, the National Aeronautics and Space Administration, and the Robert A. Welch Foundation.

[1] R. F. Stebbings, B. R. Turner, and J. A. Rutherford, J. Geophys. Res. **71**, 771 (1966).
[2] J. A. Rutherford and D. A. Vroom, J. Chem. Phys. **55**, 5622 (1971).
[3] T. F. Moran and J. B. Wilcox, J. Chem. Phys. **69**, 1397 (1978).
[4] T. F. Moran and B. P. Mathur, Phys. Rev. A **21**, 1051 (1980).
[5] J. M. Hoffman, G. H. Miller, and G. J. Lockwood, Phys. Rev. A **25**, 1930 (1982).
[6] M. Lavollée and G. Henri, J. Phys. B **22**, 2019 (1989).
[7] M. Ishimoto, M. R. Torr, P. G. Richards, and D. G. Torr, J. Geophys. Res. **91**, 5793 (1986).
[8] D. Smith and N. G. Adams, in *Topics in Current Chemistry*, edited by S. Vepřek and M. Venugopalan (Springer-Verlag, Berlin, 1980), Vol. 89, p. 1.
[9] E. G. Shelley, R. G. Johnson, and R. D. Sharp, J. Geophys. Res. **77**, 6104 (1972).
[10] J. U. Kozyra, T. E. Cravens, and A. F. Nagy, J. Geophys. Res. **87**, 2481 (1982).
[11] B. A. Tinsley, R. P. Rohrbaugh, Y. Sahai, and N. R. Teixeira, Geophys. Res. Lett. **9**, 543 (1982).
[12] M. R. Torr and D. G. Torr, Geophys. Res. Lett. **6**, 700 (1979).
[13] M. R. Torr and D. G. Torr, J. Geophys. Res. **89**, 5547 (1984).
[14] M. R. Torr, J. C. G. Walker, and D. G. Torr, J. Geophys. Res. **79**, 5267 (1974).
[15] M. R. Torr, D. G. Torr, R. G. Roble, and E. C. Ridley, J. Geophys. Res. **87**, 5290 (1982).
[16] E. E. Ferguson, F. C. Fehsenfeld, and D. L. Albritton, in *Gas Phase Ion Chemistry*, edited by Michael T. Bowers (Academic, New York, 1979).
[17] B. R. Turner, J. A. Rutherford, and D. M. J. Compton, J. Chem. Phys. **48**, 1602 (1968).
[18] M. Hamden and A. G. Brenton, J. Phys. B **22**, 2289 (1989).
[19] R. S. Gao, P. S. Gibner, J. H. Newman, K. A. Smith, and R. F. Stebbings, Rev. Sci. Instrum. **55**, 1756 (1984).
[20] L. K. Johnson, R. S. Gao, C. L. Hakes, K. A. Smith, and R. F. Stebbings, Phys. Rev. A **40**, 4920 (1989).
[21] R. S. Gao, L. K. Johnson, D. A. Schafer, J. H. Newman, K. A. Smith, and R. F. Stebbings, Phys. Rev. A **38**, 2789 (1988).
[22] B. G. Lindsay, D. R. Sieglaff, D. A. Schafer, C. L. Hakes, K. A. Smith, and R. F. Stebbings, Phys. Rev. A **53**, 212 (1996).
[23] X. Li, Y.-L. Huang, G. D. Flesch, and C. Y. Ng, J. Chem. Phys. **106**, 1373 (1997).
[24] G. D. Flesch and C. Y. Ng, J. Chem. Phys. **92**, 3235 (1990).
[25] Y. Xu, E. W. Thomas, and T. F. Moran, J. Phys. B **23**, 1235 (1990).
[26] A. D. Irvine and C. J. Latimer, J. Phys. B **24**, L145 (1991).
[27] G. D. Flesch and C. Y. Ng, J. Geophys. Res. **96**, 21 407 (1991).